Technical University of Denmark

DTU

Molten Triazolium Chloride Systems as New Aluminum Battery Electrolytes

Vestergaard, B.; Bjerrum, Niels J.; Petrushina, Irina; Hjuler, H.A.; Berg, Rolf W.; Begtrup, M.

DTU Library
Technical Information Center of Denmark

Molten Triazolium Chloride Systems as New Aluminum Battery Electrolytes

B. Vestergaard,[a] N. J. Bjerrum,[*,a] I. Petrushina,[b] H. A. Hjuler,[*,c] R. W. Berg,[a] and M. Begtrup[d]

[a] *Materials Science Group, Chemistry Department A, The Technical University of Denmark, DK-2800 Lyngby, Denmark*
[b] *Institute of General and Inorganic Chemistry, 252680 Kiev-142, Ukraine*
[c] *NKT Research Center, DK-2605 Brøndby, Denmark*
[d] *Department of Organic Chemistry, Royal Danish School of Pharmacy, DK-2100 Copenhagen, Denmark*

ABSTRACT

The possibility of using molten mixtures of 1,4-dimethyl-1,2,4-triazolium chloride (DMTC) and aluminum chloride (AlCl$_3$) as secondary battery electrolytes was studied, in some cases extended by the copresence of sodium chloride. DMTC-AlCl$_3$ mixtures demonstrated high specific conductivity in a wide temperature range. The equimolar system is most conductive and has κ values between 4.02×10^{-5} and 7.78×10^{-2} S cm^{-1} in the range from -31 to $123°C$, respectively. The electrochemical window of DMTC-containing sodium tetrachloroaluminate melts varied in the region of 2.5 to 2.2 V (150-170°C) depending on melt acidity and anode material. DMTC, being specifically adsorbed and reduced on the tungsten electrode surface, had an inhibiting effect on the aluminum reduction, but this effect was suppressed on the aluminum substrate. An electrochemical process with high current density (tens of milliamperes per square centimeter) was observed at 0.344 V on the acidic sodium tetrachloroaluminate background, involving a free triazolium radical mechanism. Molten DMTC-AlCl$_3$ electrolytes are acceptable for battery performance and both the aluminum anode and the triazolium electrolyte can be used as active materials in the acidic DMTC-AlCl$_3$ mixtures.

The development of high energy density secondary batteries, with aluminum anode as the most attractive alternative to lithium and sodium, is an important subject of research. It can be justified by low price, chemical stability, high theoretical capacity, and high energy density of the aluminum.

Depending on temperature range at least two battery systems are now being developed: a moderate temperature system with sodium chloride-aluminum chloride[1-9] or 1-butylpyridinium chloride-aluminum chloride[10-12] molten mixtures as electrolytes, and a room temperature system with molten mixtures of aluminum chloride and organic quaternary salts, usually 1-methyl-3-ethylimidazolium chloride (MEIC)[13-17] as electrolytes, the latter system being more attractive because of the wider temperature range. Despite satisfactory cycling efficiency of the aluminum anode in the MEIC electrolytes these batteries have the following disadvantages:[16,17] (*i*) low allowed current densities (<1 mA cm^{-2}); (*ii*) necessity of an ion-exchange membrane because of different composition of the anolyte and catholyte; and (*iii*) limitations in choice of cathodic materials.

Several attempts to extend electrochemical windows of the room-temperature molten electrolytes have been undertaken:[18-23] a molten MEIC-aluminum chloride mixture of nearly neutral composition obtained by NaCl addition until saturation and further a 1.5:1 molten mixture of AlCl$_3$-1,2-dimethyl-3-propylimidazolium chloride have been used as modified electrolytes.[18,19] In the first case sodium can be used as anode instead of aluminum (anodic extending) and in the second case a chlorine cathode has been realized, based on an intercalation process in graphite (cathodic extending). Unfortunately, good cycling behavior has not been found for the sodium anode because of a passivating layer.[18] Concerning the chlorine electrode, chlorine storage capacity of graphite has not been sufficient for a suitable energy density,[19] probably because of the absence of a chlorine intercalation into graphite.

Recently, aluminum-polyaniline secondary batteries have been developed[20-23] using molten acidic MEIC-AlCl$_3$ or butylpyridinium chloride-AlCl$_3$ mixtures as electrolytes. However, Günter *et al.* have determined slight dissolution of polyaniline in the acidic melts and subsequent degradation of the cathodes after 20-30 cycles.[23]

Therefore the development of new electrolyte systems for room-temperature aluminum secondary batteries is still an important field of investigation. It was natural after imidazole to study a related compound in the group of five-membered azo-heterocycles, *i.e.*, triazole.

Here, we report the conductivity and voltammetry of DMTC-AlCl$_3$ (Fig. 1) as possible secondary battery electrolytes. For the voltammetric measurements the idea of Matsunaga *et al.*[24] has been used: the electrochemical behavior of DMTC-AlCl$_3$ systems in both acidic and basic regions has been studied in a diluted state in sodium tetrachloroaluminate melts. In this way, all the processes due to DMTC became more pronounced.

Experimental

1-Methyl-1, 2, 4-triazole, synthesized and purified as described in Ref. 25 was dissolved in dry nitromethane (200 cm^3/mol). One equivalent of trimethyloxonium tetrafluoroborate[26] was added and the mixture stirred for 2 h. Fourfold dilution with dry ether, decantation, and washing with dry ether gave 93% of 1,4-dimethyl-1,2,4-triazolium tetrafluoroborate. This compound was dissolved in boiling water (0.5 cm^3/g) and 1 eq. of aqueous 5M KCl was added. Cooling to 0°C, removal of the separated KBF$_4$ by filtration, evaporation to dryness, recrystallization from ethanol-ether, and drying at 0.1 mm Hg over P$_2$O$_5$ (to remove any traces of water) gave 86% of DMTC, mp 103-104°C. The preparation of distilled aluminum chloride and dried NaCl has been described previously.[27] All sample preparation and handling took place in an argon-filled glove box (Vacuum Atmospheres Inc.), with oxygen concentration 10 ppm (monitored with a Dansensor System A/S unit).
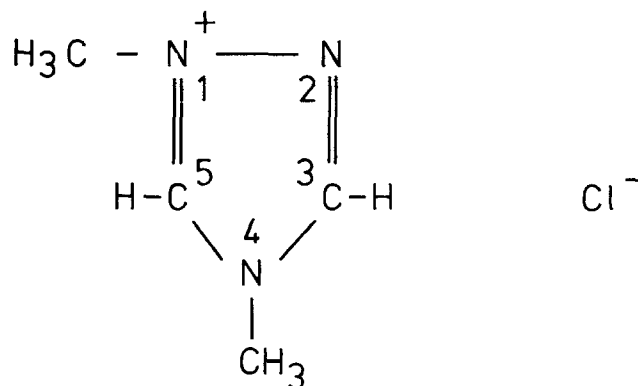

Fig. 1. DMTC = 1,4-dimethyl-1,2,4-triazolium chloride (structural formula).
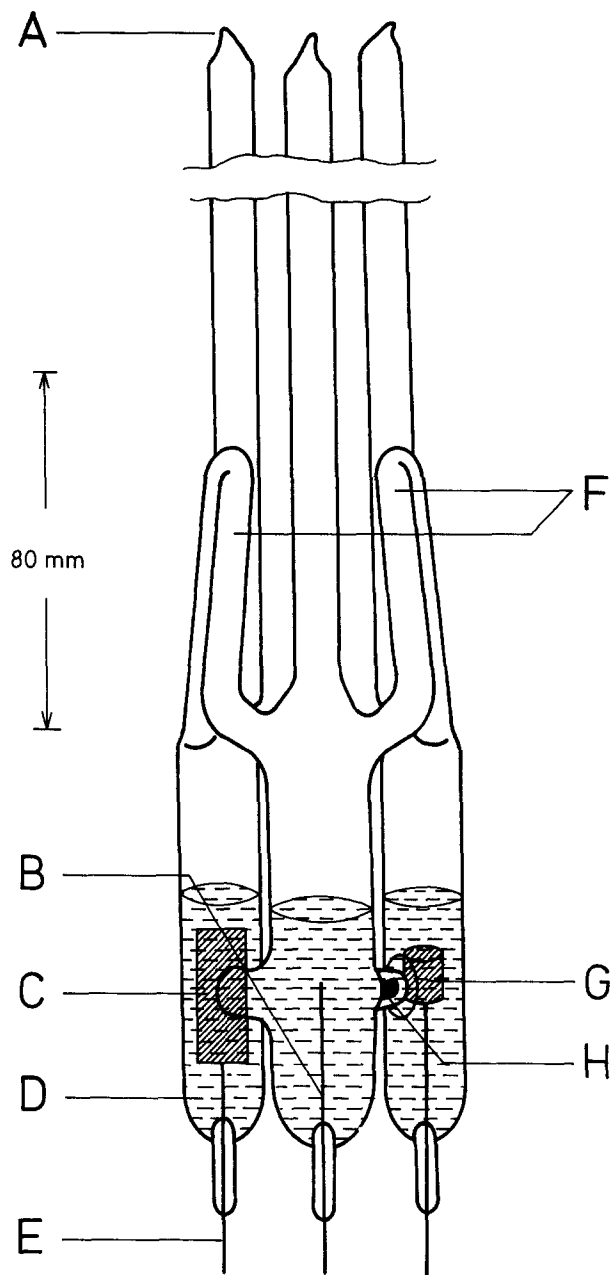
Fig. 2. Potentiometric cell with 3 chambers: (A) seal off; (B) tungsten working electrode; (C) molybdenum counterelectrode; (D) electrolyte; (E) tungsten current collectors; (F) sealed pressure equilibration tubes; (G) aluminum reference electrode; and (H) porous ceramic separator.

The same conductance cell was used for all samples, an H-type Pyrex cell with a capillary of diameter and length equal to 0.1 and 1.0 cm, respectively (the cell constant was 40.94). Tungsten wire electrodes were sealed in the bottom of cell compartments. After each addition, the cell was evacuated, filled with Ar to a pressure of 50 kPa and sealed in the upper part of one of the compartments. The conductance cell was calibrated at room temperature using the standard technique (0.1 demal aqueous KCl).[28] During the experiments the cell was immersed in a well-stirred silicone oil bath. A REX-C4 proportional temperature controller was used. The temperature was stabilized within ±0.1°C. The temperature scanning rate was 0.5°C/min. The reproducibility of conductivity values was controlled by performing two cooling and two heating scans in each concentration point. Conductance measurements were made with a Radiometer A/S (Copenhagen) Model CDM 83 conductivity meter, working at the following frequencies, which automatically changed depending on the conductiv-
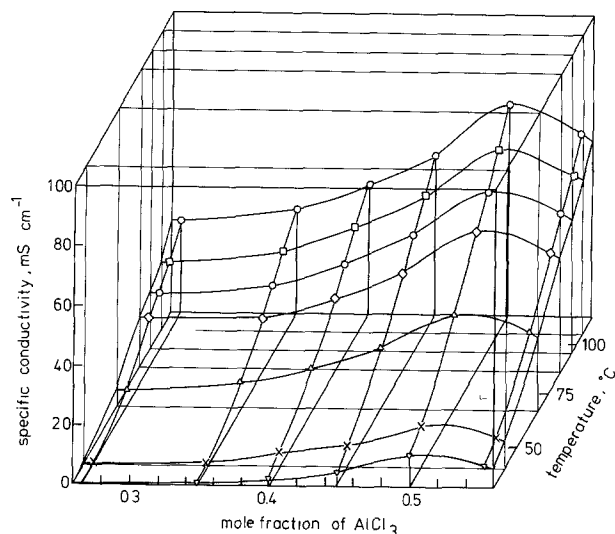

Fig. 3. Specific conductivity of DMTC-AlCl$_3$ mixtures as a function of composition and temperature (lines are made by hand).

ity: 586 Hz (below 0.13 mS cm^{-1}); 4.69 kHz (below 1.3 mS cm^{-1}); and 50 kHz (below 13 mS cm^{-1}).

Cyclic voltammetry was performed in a double H-type three-compartment Pyrex cell (Fig. 2). A tungsten wire working electrode (0.36 cm^2), a molybdenum foil counterelectrode, and an aluminum reference electrode (in 0.6 NaCl − 0.4 AlCl$_3$ melt) were used. Also, the electrochemical cell was sealed under 50 kPa of argon after each addition. The same silicone oil bath and temperature controller were used. Voltammetric measurements were carried out with a Schlumberger Model SI1286 electrochemical interface. The CORRSOFT ERIC System 2 software program was used to control the SI1286.

Results and Discussion

Conductivity measurements.—Here, the concentration of binary mixtures of DMTC and aluminum chloride is expressed as mole fraction of AlCl$_3$ (X). As in Ref. 29, our measurements were carried out mainly in the basic concentration region ($X < 0.5$), because of high melting points and low conductivities of AlCl$_3$-rich compositions.

For $X > 0.35$ all studied compositions were liquid at room temperature, *i.e.*, their melting points were markedly lower than for the 1,3-dimethylimidazolium chloride (DMIC)-aluminum chloride mixtures and at $X = 0.5$ even lower than for the MEIC-AlCl$_3$ melt.[29]

The specific conductivity of the DMTC-AlCl$_3$ system in the temperature range of 29.3-114.0°C is shown in Fig. 3, and the corresponding data are given in Table I. As for N-ethylpyridinium chloride-AlCl$_3$[30] and the 1,3-alkylimidazolium chloride-AlCl$_3$[29] melts, the specific conductivity of DMTC-AlCl$_3$ mixtures is strongly dependent on the composition of the melt. For all systems, equimolar mixtures have peak conductivity values. The equimolar DMTC-AlCl$_3$ conductivity is close to the corresponding MEIC-AlCl$_3$ mixture.

Table I. Specific conductivity κ (mS cm^{-1}); of the DMTC-AlCl$_3$ mixtures.

X of AlCl$_3$ t (°C)	0.268	0.348	0.399	0.448	0.500	0.553
29.3	—	0.798	2.231	4.753	10.64	7.369
39.9	0.950	1.933	4.585	7.533	14.33	10.64
57.7	2.121	5.527	9.676	15.53	26.27	20.83
67.0	5.199	8.475	13.69	20.36	31.74	26.65
76.5	10.64	12.26	18.22	25.93	38.71	32.77
86.0	16.40	16.77	23.38	32.00	46.13	39.46
95.2	19.08	21.73	29.15	38.50	53.68	46.36
104.7	22.71	27.23	35.25	45.61	61.82	53.35
114.0	29.87	33.86	42.15	52.81	70.21	61.14

Table II. Least squares fit parameters for specific conductivities according to Eq. 1.[a]

X of $AlCl_3$	κ_0 (mS cm^{-1})	A [mS cm^{-1} (°C)$^{-1}$]	B [mS cm^{-1} (°C)$^{-2}$]	t_{min} (°C)	t_{max} (°C)	No. of points	R^2
0.268	11.0001 (6000)	0.47634 (630)	5.5249 (2000)	35	110	32	0.99530
0.348	13.7711 (3400)	0.45213 (240)	3.85476 (9000)	30	120	30	0.99929
0.399	19.8544 (1000)	0.53710 (80)	3.68924 (3000)	30	120	29	0.99995
0.448	28.0325 (3100)	0.62292 (220)	3.057 (90)	40	125	29	0.99968
0.500	40.7721 (6900)	0.75757 (370)	3.47999 (4000)	−15	125	77	0.99922
0.553	35.2458 (5000)	0.67948 (350)	2.48172 (10000)	30	125	30	0.99933

[a] Standard deviation on last digits of A and B parameters are given in parantheses. R^2 is the correlation index, which was calculated, using the equation

$$R^2 = \left[\sum_{i=1}^{n}(\kappa_i - \overline{\kappa})^2 - \sum_{i=1}^{n}(\kappa_i - \hat{\kappa}_i)^2\right]\bigg/\sum_{i=1}^{n}(\kappa_i - \overline{\kappa})^2 \quad \text{with} \quad \overline{\kappa} = \frac{1}{n}\sum_{i=1}^{n}\kappa_i$$

Experimental values of specific conductivity, κ, for each composition were least squares fit to equations of the form

$$\hat{\kappa} = \kappa_0 + A(t - t_0) + B(t - t_0)^2 \qquad [1]$$

where $\hat{\kappa}$ is the estimated regression value, κ_0 is the regression constant, t is the temperature in centigrade and t_0 is a fixed reference point (set to 80°C). The values of the parameters of Eq. 1 are given in Table II (with temperature ranges).

According to Fig. 4, and unlike the DMIC-AlCl$_3$ and MEIC-AlCl$_3$ melts, the DMTC-AlCl$_3$ mixture at X = 0.5 demonstrates an obvious non-Arrhenius behavior, with a glass formation temperature close to zero. But the most important property for battery applications is that the equimolar DMTC-AlCl$_3$ melt has a sufficiently high conductivity down to −30°C. The described temperature dependence of the specific conductivity can be explained by assuming that the pure DMTC melt (as for alkylpyridinium and alkylimidazolium chlorides) is a strongly associated liquid that forms an ionic dissociated compound at X = 0.5. Therefore addition of aluminum chloride to the DMTC melt must be followed by destruction of the associates, entropy growth[31] and subsequent increase of electroconductivity with pronounced glass-forming tendency. A similar behavior must be at the other side of the phase diagram, as aluminum chloride is dimerized and almost nonconductive in the liquid state. The addition of a strongly polarizing ion, such as Li$^+$, may have an opposite effect, forming associates and lowering the entropy as well as the conductivity. This assumption is in good agreement with the experimental conductivity data measured by Fannin *et al.*[29] for the MEIC-AlCl$_3$ with small LiCl additions and with the results obtained by Matsunaga *et al.*[24] on the LiCl influence on the electrochemical behavior of the $AlCl_4^-$ anion in MEIC-NaCl-AlCl$_3$ melts.[24]

Voltammetric measurements.—Voltammetric curves for the melts of neutral or slightly basic sodium tetrachloroaluminate with 1 and 2 mole percent (m/o) additions of DMTC are shown in Fig. 5 (obtained with a tungsten electrode). In the presence of DMTC, the potential of aluminum electroreduction becomes almost 100 mV more negative than for the pure NaAlCl$_4$ electrolyte. Moreover four new waves appear on the voltammetric curves: oxidation waves (I and II) with initial potentials of 1.82 and 2.29 V and reduction waves (III and IV) with initial potentials of 2.15 and 1.09 V, the wave parameters depending on the DMTC concentration. Wave I disappears during cycling in a potential range more positive than 1.0 V (Fig. 6) and wave III, being obviously an electroreduction of the product of process II, has a strong passivating effect on the aluminum reduction and oxidation: both of them are suppressed when negative polarization follows the positive one (Fig. 7). Peak current (I_p) and peak potential (E_p) of wave III depend linearly on the square root of the potential scanning velocity.

In the slightly acidic melt the electrochemical behavior of DMTC (added in the form of a 0.447 DMTC-0.553 AlCl$_3$ melt) differs very much from that in the basic melt (Fig. 8B). The aluminum electroreduction initial potential, as in the basic melt, becomes 100 mV more negative but, unlike for the basic triazolium melts and for the acidic imidazolium melts, the wave of aluminum electro-oxidation disappears, *i.e.* it is suppressed by DMTC. Furthermore, new high velocity electrochemical processes, involving DMTC, can be seen in the voltammetric curves (waves V and VI in Fig. 9). Both waves have the same initial potential, 0.344 V, but the peak potential difference is distinct and exceeds 1 V, decreasing with the temperature (Fig. 10) and scan velocity. For both waves peak current densities are unusually high (even at the lowest experimental temperature and potential scan velocity, *i.e.* 153.3°C and 8.3 mV s^{-1}, peak V current density is 66 mA cm^{-2}). The i_{pa}/i_{pc} value approaches unity when the temperature decreases (Fig. 10). Both peak parameters are reproducible (cycling tens of times), including low potential scan velocity conditions. The peak currents and potentials depend linearly on the square root of the scan velocity (Fig. 11). Both triazolium processes depend on the electrode material: triazolium reduction is suppressed at the aluminum electrode and the wave of aluminum electro-oxidation appears on the voltammetric curve (Fig. 12).
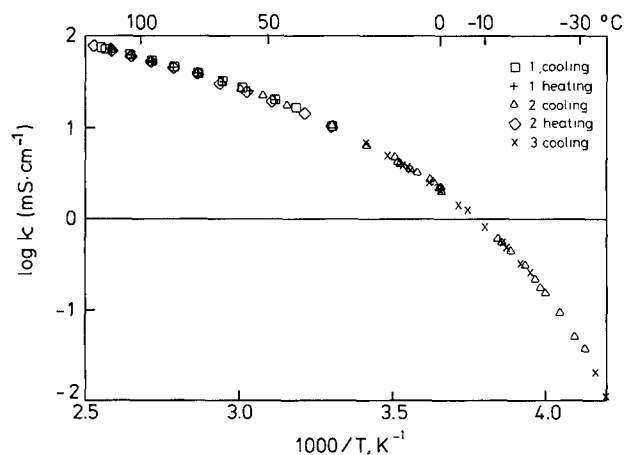

Fig. 4. Logarithmic plot of the specific conductivity in the equimolar DMTC-AlCl$_3$ mixture *vs.* the reciprocal temperature.
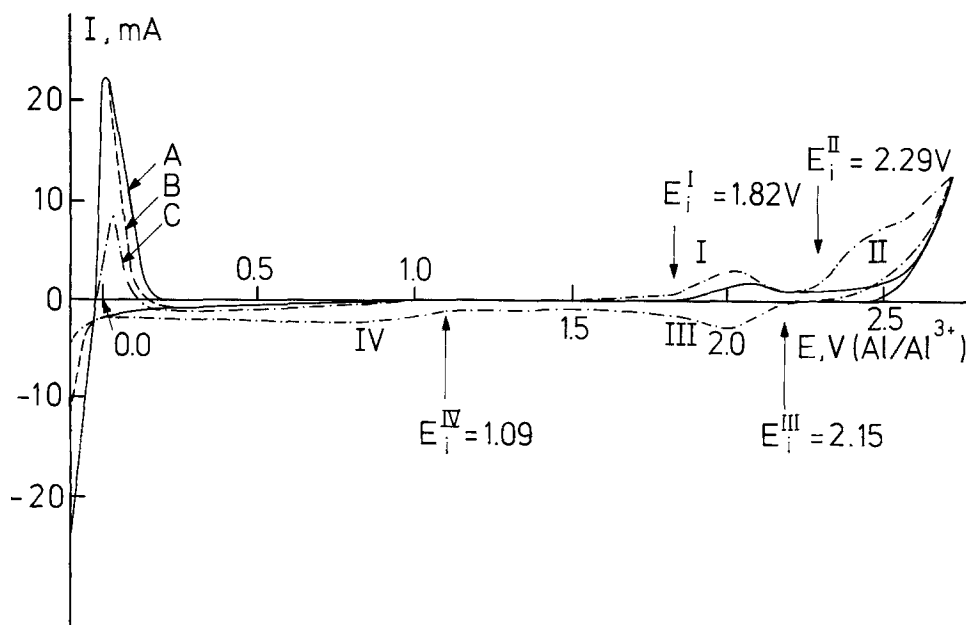
Fig. 5. Cyclic voltammograms with tungsten electrode at 169°C and 2 V min^{-1} vs. electrolyte: (A) NaCl:AlCl$_3$ (0.5000;0.5000); (B) NaCl:AlCl$_3$:DMTC (0.4951: 0.4951:0.0098); (C) NaCl:AlCl$_3$: DMTC (0.4903:0.4903:0.0194). E_i^I- E_i^{IV} indicates where wave I to IV start.

Anodic oxidation of NaAlCl$_4$ (oxidation of the tetrachloroaluminate ion[19]) is not effected by DMTC-AlCl$_3$ addition (Fig. 8).

From the results of the voltammetric measurements we conclude that in acidic and basic regions triazolium chloride has a significant effect on the electrochemical behavior of the sodium tetrachloroaluminate melt. Similar to imidazolium chloride,[17,24] DMTC has an inhibiting effect on the aluminum electroreduction. However, contrary to the behavior of imidazolium melts, the aluminum electro-oxidation on tungsten is suppressed in acidic melts, while being slightly affected in basic melts (mainly because of the higher aluminum reduction polarization and the fixed potential scanning region (Fig. 6).

In the basic electrolyte the strong passivating effect of the processes II-III on the electrochemical behavior of aluminum can be explained by the appearance of a lower conductive passivating surface layer (probably polymeric, taking into account the well-known properties of the benzotriazole.[32] Dependence of the II-III peak potentials on the square root of the potential scan velocity, showing ohmic control of this process,[33] is in agreement with our explanation.

Wave I can be ascribed to the oxidation of Cl$^-$ ions in slightly basic melts[19] and the disappearance of wave I when cycling in the high positive potential part of the potential window can be explained by the passivating effect of the wave III surface layer.
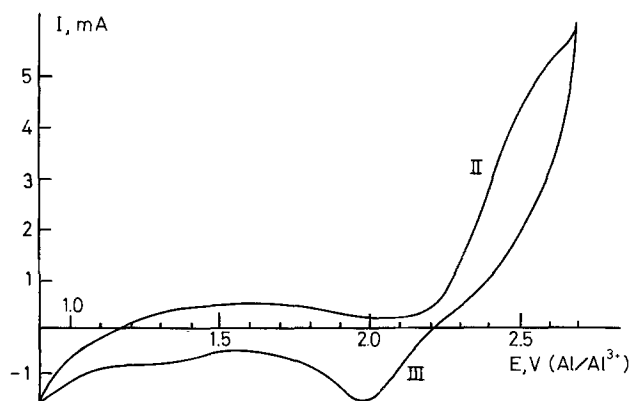
Wave IV can be ascribed to the reduction of the triazolium ion in the basic melt, similar to the imidazolium ion reduction in MEIC molten mixtures.[17]

In the acidic electrolyte, peak current densities for waves V and VI are higher than those expected even for a reversible electrochemical reaction (if the diffusion coefficient is supposed to be ~10^{-7} cm^2 s^{-1} and the diffusional layer is 10^{-2} cm). This phenomenon may be explained as an electroreduction of specifically adsorbed triazolium cations with formation of a stable adsorbed radical, and subsequent oxidation of this radical according to the equation

$$\qquad\qquad\qquad\qquad [2]$$
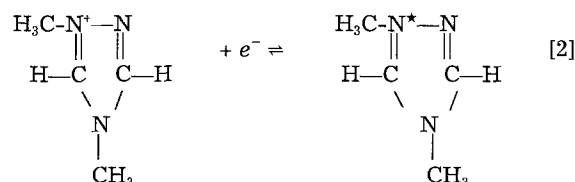
This explanation is in good agreement with R. A. Osteryoung's observations concerning the remarkable stabilization of aromatic amine radical cations in AlCl$_3$-NaCl melts, even at 175°C, and the dependence on the melt acidity.[34] In the present case ohmic control can be ascribed to the lower conductivity of the DMTC-rich surface layer. The tria-
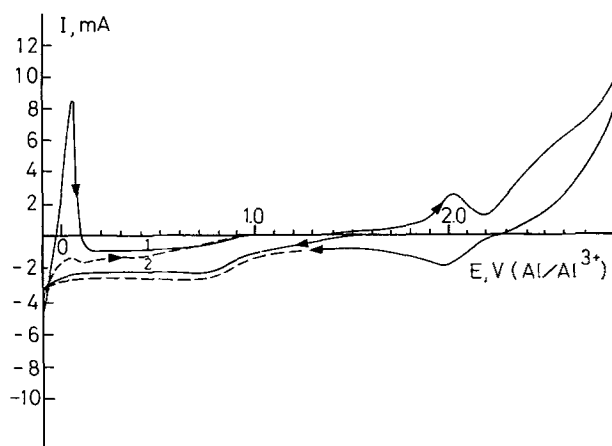

Fig. 6. Cyclic voltammogram performed with tungsten electrodes at 169.3°C and 2 V min^{-1} for NaCl:AlCl$_3$:DMTC (0.4903:0.4903: 0.0194). Second potential scan in the anodic part of the electrochemical window.

Fig. 7. Cyclic voltammogram performed with tungsten electrodes at 169.3°C and 2 V min^{-1} for NaCl:AlCl$_3$:DMTC (0.4903:0.4903: 0.0194). The first and second potential scans.
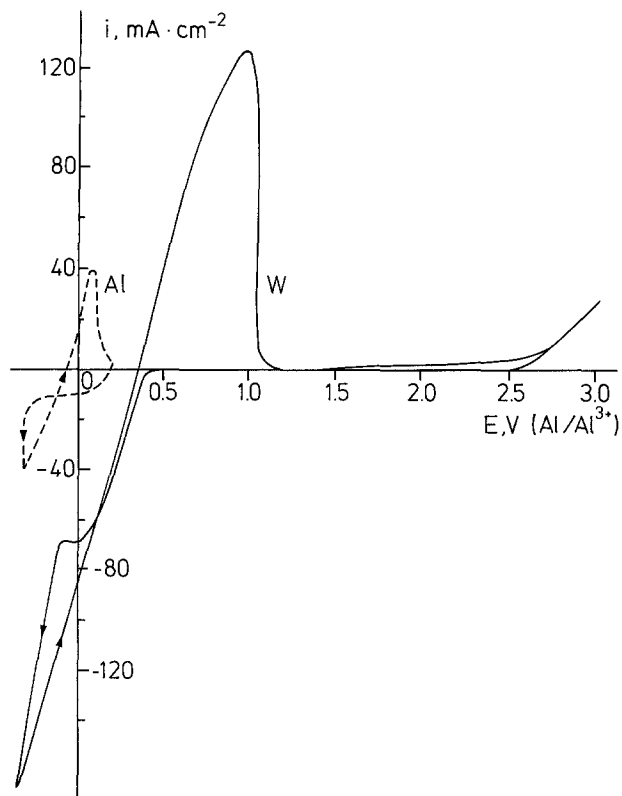
Fig. 8. Cyclic voltammogram performed with tungsten electrodes at 165°C and 1 V min⁻¹ for (A) NaCl:AlCl₃ (0.5000:0.5000), and (B) NaCl:AlCl₃:DMTC (0.4763:0.5025:0.0212).

zolium ion electrochemical behavior depends on the electrode material used. That is why it is possible to have a rechargeable aluminum electrode when we use pure aluminum in acidic melts, hence suppressing triazolium ion reduction.

In conclusion, DMTC-AlCl₃ melts can be used as secondary battery electrolytes with aluminum as anode in both basic and acidic mixtures in a wide temperature range.

However, the most important property of the studied electrolytes is the electrochemical activity of the triazolium chloride at potentials close to the aluminum reduction-oxidation processs in the acidic melts. The utilization of reaction 2 as an anode (instead of aluminum) in secondary batteries is promising because of higher reversibility, current density, and theoretical capacity. The combination of the triazolium process with such cathodic materials as polymers in secondary battery systems moreover has the fol-
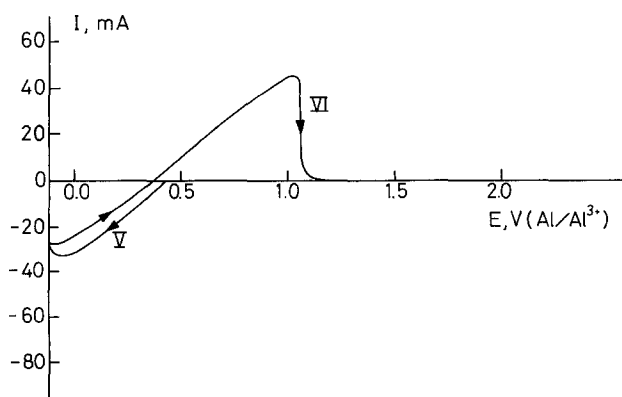

Fig. 9. Cyclic voltammogram performed with tungsten electrodes at 170.3°C and 2 V min⁻¹ for NaCl:AlCl₃:DMTC (0.4763:0.5025: 0.0212). Potential scan without aluminum wave.
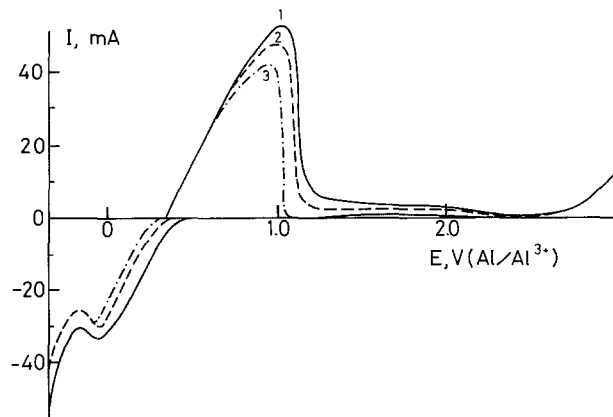

Fig. 10. Temperature dependence of the tungsten electrodes electrochemical behavior at 2 V min⁻¹ in NaCl:AlCl₃:DMTC (0.4763: 0.5025:0.0212. Scan 1, 170.4°C; scan 2, 161.3°C; scan 3, 153.9°C.

lowing advantages: (*i*) absence of an ionic-exchange membrane; (*ii*) possibility of thin-layer battery design; and (*iii*) possible environmental advantage of using organic materials in the battery.
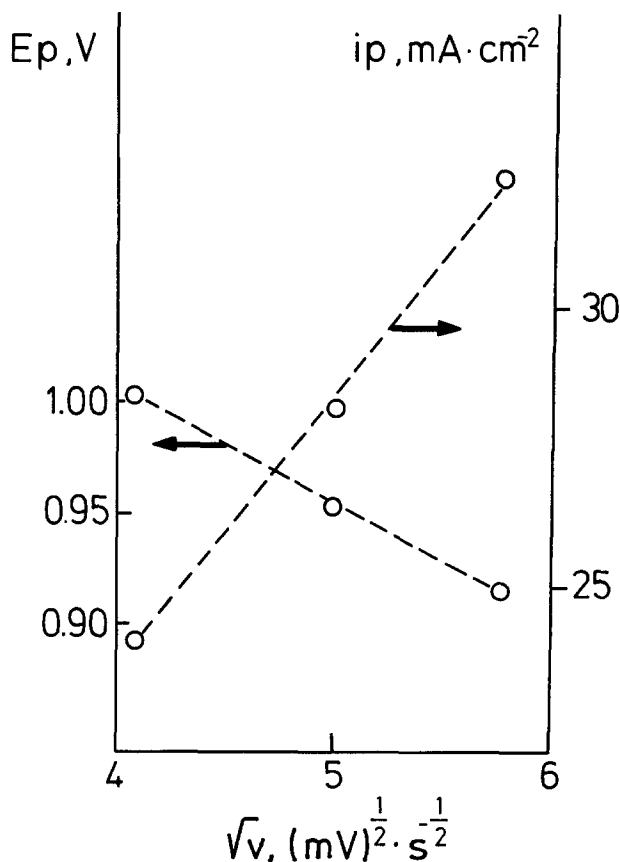
Acknowledgments

Fig. 11. Peak current and potential *vs.* the square root of the potential scan rate for wave VI (Fig. 9).
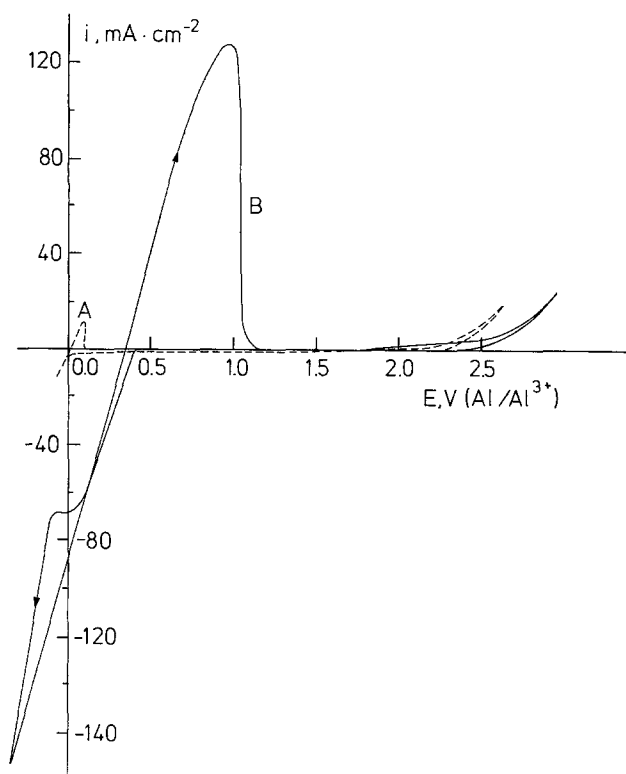
Fig. 12. Cyclic voltammogram obtained with tungsten (W) and aluminum (Al) electrodes at 165°C and 1 V min⁻¹ for NaCl:AlCl₃: DMTC (0.4763:0.5025:0.0212).

REFERENCES

1. Danish Pat. 154180.
2. H. A. Hjuler, R. W. Berg, and N. J. Bjerrum, *Power Sources,* **10,** 1 (1985). (Proceedings of the 14th International Power Sources Symposium.)
3. H. A. Hjuler, S. von Winbush, R. W. Berg, and N. J. Bjerrum, *This Journal,* **136,** 901 (1989).
4. H. A. Hjuler, J. E. Engell, J. Høj, and N. J. Bjerrrum, *Proceedings, The 7th Australian Electrochemistry Conference,* p. 73 (1988).
5. S. Takamashi and N. Koura, *Keikinzoku,* **35,** 630 (1985).
6. S. Takahashi, N. Koura, and N. Yoneda, *Denki Kagaku,* **52,** 244 (1984).
7. N. Koura, Y. Kaneta, and N. Takami, *ibid.,* **52,** 830 (1984).
8. N. Takami and N. Koura, *ibid.,* **53,** 890 (1985).
9. N. Takami and N. Koura, *ibid.,* **54,** 288 (1986).
10. S. Takahashi, N. Koura, and R. Nakajima, *ibid.,* **54,** 257 (1986).
11. S. Takahashi, N. Koura, and R. Nakajima, *ibid.,* **54,** 263 (1986).
12. N. Takami and N. Koura, *This Journal,* **136,** 730 (1989).
13. European Pat. 404179.
14. Japanese Pat. 89296572.
15. S. E. Mancini and F. M. Donahue, in *Proceedings of the Seventh International Symposium on Molten Salts,* C. L. Hussey, S. N. Flengas, J. S. Wilkes, and Y. Ito, Editors, PV 90-17, p. 389, The Electrochemical Society Proceedings Series, Pennington, NJ (1990).
16. J. S. Wilkes, J. A. Levisky, J. S. Landers, C. L. Hussey, R. L. Vaughn, D. A. Floreani, and D. J. Stech, Frank J. Seiler Laboratory Technical Report FJSRL-TR-81-011, ADA 107,989 (Oct. 1981).
17. B. J. Piersma and J. S. Wilkes, Frank J. Seiler Laboratory Technical Report FJSRL-TR-82-0004, ADA 122, 840 (Sept. 1982).
18. C. Scordilis-Kelley, J. Fuller, R. T. Carlin, and J. S. Wilkes, *This Journal,* **139,** 694 (1992).
19. P. R. Gifford and J. B. Palmisano, *ibid.,* **135,** 650 (1988).
20. N. Koura and H. Ejiri, *Kenkyu Hokoku-Asahi Garasu Zaidan,* **56,** 333 (1990).
21. N. Koura and H. Ejiri, in *Proceedings of the Seventh International Symposium on Molten Salts,* C. L. Hussey, S. N. Flengas, J. S. Wilkes, and Y. Ito, Editors, PV 90-17, p. 785, The Electrochemical Society Proceedings Series, Pennington, NJ (1990).
22. Japanese Pat. 88264878.
23. F. Günter and J. Desilvestro, in *Third International Symposium on Molten Salt Chemistry and Technology,* Abstracts, p. 7 (1991).
24. M. Matsunaga, T. Miwa, Y. Inoue, and K. Hosokawa, *Mater. Sci. Forum,* **70-73,** 473 (1991).
25. M. Begtrup and P. Larsen, *Acta Chem. Scand.,* **44,** 1050 (1990).
26. *Organic Syntheses,* R. E. Benson, Editor, Vol. 51, p. 142, Wiley & Sons, New York (1971).
27. R. W. Berg, H. A. Hjuler, and N. J. Bjerrum, *Inorg. Chem.,* **23,** 557 (1984).
28. G. Jones and B. Bradshaw, *J. Am. Chem. Soc.,* **55,** 1780 (1933).
29. A. A. Fannin, Jr., D. A. Floreani, L. A. King, J. S. Landers, B. J. Piersma, D. J. Stech, R. L. Vaughn, J. S. Wilkes, and J. J. Williams, *J. Phys. Chem.,* **88,** 2614 (1984).
30. R. A. Carpio, L. A. King, R. E. Lindstrøm, J. C. Nardi, and C. L. Hussey, *This Journal,* **126,** 1644 (1979).
31. B. F. Markov, *Thermodynamics of Molten Salts* (Russian), Naukova Dumka, Kiev (1974).
32. D. Tromans and R. Sun, *This Journal,* **138,** 3235 (1991).
33. A. J. Calandra, N. R. de Tacconi, R. Pereiro, and A. J. Arvia, *Electrochim. Acta,* **19,** 901 (1974).
34. H. L. Jones and R. A. Osteryoung, *J. Electroanal. Chem.,* **49,** 281 (1974).